Nuclear Materials and Energy 12 (2017) 1061–1066

Contents lists available at ScienceDirect

Nuclear Materials and Energy

journal homepage: www.elsevier.com/locate/nme

Stability of divertor detachment

S.I. Krasheninnikov[d,*], A.S. Kukushkin[a,b], A.A. Pshenov[a,b], A.I. Smolyakov[c], Yanzeng Zhang[d]

[a] Kurchatov Institute, Kurchatov sq. 1, 123182 Moscow, Russia
[b] NRNU MEPhI, Kashirskoe sh. 31, 115409 Moscow, Russia
[c] University of Saskatchewan, 116 Science Place, Saskatoon, SK S7N 5E2, Canada
[d] University California San Diego, 9500 Gilman Drive, La Jolla, CA 92093-0411, USA

ARTICLE INFO

Article history:
Received 27 June 2016
Revised 2 November 2016
Accepted 18 January 2017
Available online 10 March 2017

Keywords:
Divertor detachment
Stability
Bifurcation
Impurity
Anomalous transport
Recycling

ABSTRACT

The 2D simulations of edge plasma transport show that unlike some earlier publications, the impurity radiation loss *per se* does not cause the bifurcation-like transition to detached divertor regime. However, for the case where anomalous plasma transport is increasing with advancement to detachment, like it was recently observed experimentally, the transition to detachment exhibit the bifurcation-like character. Some other plausible reasons for similar bifurcation-like evolution to detachment are discussed. It is demonstrated that the current convective instability can be triggered in detached inner divertor plasma for the condition when outer divertor is still attached. This can explain the fluctuations of radiation loss observed recently experimentally for similar conditions. The self-sustained oscillations observed recently in numerical simulations and related to the interplay of the thermal force effects in impurity transport and impurity radiation loss are further investigated. It is shown that for some conditions these oscillations are ubiquitous, since no stable solutions possible.

1. Introduction

Large heat and particle fluxes on divertor targets, envisioned in future magnetic fusion reactors, make the detached regime of divertor operation in future reactors virtually mandatory. Detached divertor regimes are characterized by large radiation loss and a "rollover" of plasma flux to the targets [1,2]. Experimental data show that the transition to detachment can have bifurcation-like character while the operation in the detached regime can exhibit strong fluctuations of divertor plasma parameters (e.g. see Refs. 3–5). Both simplified analytical and semi-analytical models and numerical simulations also demonstrate the possibilities of such phenomena (e.g. see Refs. 6–8). However, often such simplified analytical and semi-analytical models are missing important ingredients and their results are not supported by more sophisticated numerical simulations. On the other hand the lack of the first principal models for the description of some complex phenomena (e.g. anomalous cross-field plasma transport, hydrogen retention in plasma facing components (PFCs), etc.) forces to make some *ad hoc* assumptions in the simulation set up, which can result in disagreement with experimental observations or lead to wrong conclusions. For example, in numerical simulations it is often assumed that anomalous plasma transport coefficients are fixed. However, experiment shows that anomalous cross-field transport in the scrape off layer (SOL) changes significantly in the process of transition to detached regime in both L- and H- modes [9], which, as we will see below, can be crucial for the processes of transition to detached divertor regime. Thus, it is fair to say that the applicability of theoretical and computational results predicting the SOL plasma parameter bifurcations and fluctuations and, therefore, the physics of experimentally observed bifurcations and fluctuations are still not clear. It is also plausible that some new phenomena, which are not accounted for in existing theoretical/computational models, are responsible for these experimental observations.

In this paper we present the results of our studies on the transition to divertor detachment and possible origin of the fluctuations of plasma parameters in detached state. The remaining of the paper is organized as follows: In Section 2, based on 2D simulations of edge plasma transport, we show that unlike some earlier theoretical publications (e.g. see Refs. [6,7]), the impurity radiation loss *per se* does not cause the bifurcation-like transition to detached divertor regime (at least for a DIII-D-size tokamak). However, for the case where anomalous plasma transport is increasing with advancement to detachment, like it was observed experimentally in Ref. [9], the transition to detachment exhibit the

* Corresponding author.
E-mail address: skrash@mae.ucsd.edu (S.I. Krasheninnikov).

http://dx.doi.org/10.1016/j.nme.2017.01.022

bifurcation-like character. We also discuss other plausible reasons for similar bifurcation-like evolution to detachment (e.g. plasma recycling). In Section 3 we show that the current convective instability can be triggered in detached inner divertor plasma for the condition when outer divertor is still attached. This can explain the fluctuations of radiation loss observed in Ref. [5] for similar conditions. In Section 4 we further investigate self-sustained oscillations observed in numerical simulations [8] and related to the interplay of the thermal force effects in impurity transport and impurity radiation loss. We show that for some conditions these oscillations are ubiquitous, since no stable solutions (both homogeneous and inhomogeneous) possible. Finally, in Section 5 we summarize our main findings.

2. Transition to detached divertor regime

It is a well-established fact [2,10] that the rollover of plasma flux to the target due to plasma volumetric recombination starts when the ratio q_{rec}/P_{up}, falls below some critical value (here q_{rec} is the specific energy flux into hydrogen recycling region and P_{up} is the upstream plasma pressure). Therefore, all processes, which can decrease q_{rec} (e.g. increase of anomalous cross field plasma transport and impurity radiation loss) and increase P_{up} (e.g. increase of plasma density in SOL due to gas puff, outgassing of the PFCs, and plasma flux from the core), can facilitate detachment process. Moreover, the synergistic effects of varying plasma parameters in the course of detachment and the processes leading to the decrease of q_{rec} and increase of P_{up} can result in abrupt, bifurcation-like, transition to detachment.

On the other hand, the results of some previous theoretical studies (e.g. see Refs. [6,7]) suggest that the bifurcation-like phenomena can be solely related to thermal instability caused by some particular geometrical features and temperature dependence of impurity radiation loss. However, these results are based on simplified models, which do not account for many effects, which, in practice, can significantly alter the conclusions following from these models.

In order to sort out an impact of impurity only on the transition to detachment but go beyond some simplified semi-analytic models like those used in Refs. [6,7], we use 2D edge plasma transport code SOLPS4.3 [11]. Similar to Ref. [2], we adopt DIII-D like magnetic configuration and geometry of the PFCs. Our simulation domain occupies some part of the core plasma, SOL, and divertor regions, the energy flux in our domain, Q_{edge}, was 8 MW, the cross-field particle and heat diffusivities were set constant in a whole computational domain, $D_\perp = 0.3\mathrm{m}^2/\mathrm{s}$, $\chi_\perp^{(e,i)} = 1\mathrm{m}^2/\mathrm{s}$. (see Ref. [12] for details of the set up and the results of the simulations). We use a "closed box" model for both deuterium plasma and impurity assuming given number of deuterium, N_D, and neon impurity, N_{Ne}, (both neutrals and ions) within the domain and instantaneous 100% recycling on the PFCs. Such model is often used (e.g. see Ref. [2]) for the modeling of high-recycling regimes where puffing and pumping effects are negligible in comparison with natural plasma recycling on the PFCs. It allows obtaining natural distribution of edge plasma parameters and their response on input parameters (e.g. Q_{edge}) including bifurcations and hysteresis effects, which are difficult to follow for other settings (e.g. by using plasma density at the core-edge interface as an input parameter). We notice that unlike simplified models used in Refs. [6,7], where impurity transport was actually ignored, our 2D simulations account for the dynamics of both neutral and charged states of impurity. We fix $N_D = 3.5 \times 10^{20}$ and vary N_{Ne} in order to observe any signs of the thermal instability (e.g. bifurcation-like dependence of divertor plasma parameters onN_{Ne}). However, no such effects were found. For example, on Fig. 1a one can see smooth dependence of maximum electron temperature at in outer divertor, T_e^{max}, and the

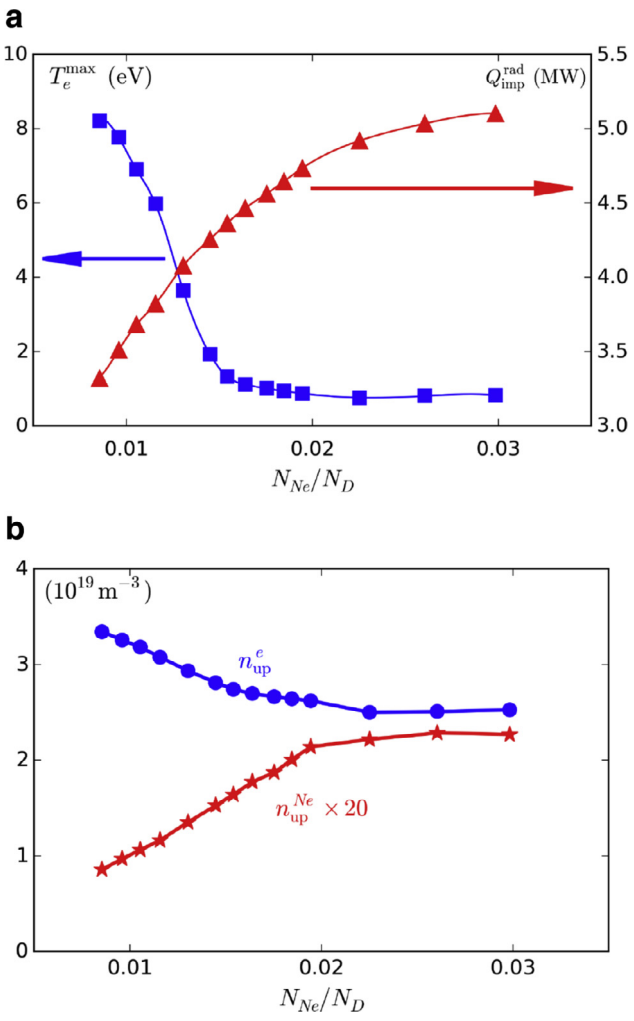

Fig. 1. The dependencies of: a) maximum electron temperature at in outer divertor, T_e^{max}, and the Neon radiation loss, Q_{imp}^{rad}, and b) upstream electron, n_{up}^{e}, and Neon, n_{up}^{Ne}, densities on the ratio N_{Ne}/N_D found from 2D numerical simulation of the DIII-D-like edge plasma with SOLPS.

Neon radiation loss, Q_{imp}^{rad}, on the ratio N_{Ne}/N_D (more results can be found in Ref. [12]). The reason for the absence of any traces of thermal instability caused by impurity radiation loss is the following. Even though the amount of impurity in the computational domain increases, when detachment proceeds a low temperature region starts to develop in the divertor volume, leaving upstream plasma parameters (e.g. upstream electron, n_{up}^{e}, and impurity, n_{up}^{Ne}, densities) virtually at some saturated level (e.g. see Fig. 1b). This cold plasma practically does not radiate, and with increasing impurity inventory in the computational domain an increasingly larger percentage of available deuterium and impurity is residing there, which saturates overall impurity radiation loss. Thus, cold region works as a stabilizing reservoir: an increase of the radiation loss increases the volume of cold region, which stores an excess of impurity and prevents further plasma cooling.

However, these findings do not mean that some meso-scale thermal instability, driven by impurity radiation but not directly affected by the presence of cold divertor plasma reservoir, cannot develop (e.g. see Ref. [8]). It is plausible that some "positive feedback" caused by plasma transport and plasma-PFCs interactions can result in the bifurcation phenomena and/or fluctuation of plasma parameters. As an example, we consider how the variation of cross-field plasma transport coefficients can alter the dynamics

of the transition to detachment. Following experimental results of Ref. [9], let assume that anomalous cross-field plasma transport coefficients are increasing in a whole domain when detachment conditions approaching. As a result, q_{rec} will go down while plasma density in the SOL will be spreading in radial direction and n_{up} decreases. However, the reduction of n_{up} increases plasma density gradient between the core and SOL plasmas, which, along with increasing anomalous transport coefficients, will increase plasma flux from the core into the SOL and, correspondingly push both n_{up} and P_{up} up. (We should notice here that the number of deuterium in the core is much larger than that in the SOL and divertor volumes, so that even small depletion of core plasma particles and channeling them through separatrix into SOL, will have a large impact on divertor plasma parameters) Simultaneously the ratio q_{rec}/P_{up}, which controls detachment process, will decrease promoting both deeper detachment and further increase of edge plasma transport coefficients, creating a "positive feedback", which can result in the bifurcation-like transition to detachment.

Qualitatively an impact of such "positive feedback" can be demonstrated, assuming plasma pressure balance between upstream and divertor regions (this approximation can only be justified for attached case [2]), with simple model based on the equations describing cross-field, parallel, and target energy balances:

$$\chi_\perp(T_d)\frac{n_{up}T_{up}A}{\Delta} = Q_{edge},\ \chi_{||}(T_{up})T_{up} = \frac{qQ_{edge}}{2\Delta},$$
$$\frac{n_{up}T_{up}}{(T_dM)^{1/2}}(E_{ion}+\gamma T_d) = \frac{Q_{edge}}{\pi R\Delta\sin(\Psi)}, \quad (1)$$

where T_{up} and T_d are the upstream and divertor plasma temperatures, A and R are the separatrix surface area and tokamak major radius, Δ is the SOL width, $\chi_{||}(T_{up}) \propto T_{up}^{5/2}$ is the parallel electron heat conduction, M is the ion mass, Ψ is the pitch angle of the magnetic field, γ is the heat transmission coefficient, q is the safety factor, and E_{ion} is the hydrogen ionization cost (for simplicity we neglect impurity radiation loss). After some algebra, from Eq. (1) we find the following equation determining the dependence $T_d(n_{up})$:

$$F(T_d) \equiv T_d^{1/2}\{\chi_\perp(T_d)\}^{-5/9}(E_{ion}+\gamma T_d)^{-1} = Cn_{up}^{14/9}, \quad (2)$$

where C is a constant determining, in particular, by Q_{edge} and geometrical parameters. From Eq. (2) we see that even for relatively large T_d ($T_d \tilde{>} E_{ion}/\gamma$) the left hand side of Eq. (2) can saturate with decreasing T_d, providing that the expression $\chi_\perp(T_d)T_d^{9/10}$ at some $T_d \tilde{<} T_d^{crit}$ starts to increase with decreasing T_d. As a result, for $n_{up} \tilde{>} n_{up}^{crit} \equiv (F(T_d^{crit})/C)^{9/14}$ no attached solution is possible and divertor abruptly goes into detached regime.

This qualitative physical picture of the bifurcation-like transition to detachment was confirmed by 2D edge plasma transport simulation with SOLPS. To mimic an increase of cross-field plasma transport coefficients, TC, in the SOL and divertor region, while detachment approaches, we assume that $TC = TC_0\{1 + (K-1)H(T_{TC}-T_{osp})(T_{TC}-T_{osp})/(T_{TC}-1)\}$, where TC_0 is the transport coefficient for the conditions far from detachment, H(x) is the Heaviside function, T_{osp} is the electron temperature, in eV, at the outer strike point, T_{TC} is some critical temperature, in eV, below which an increase of TC starts, K is the cumulative increase of TC for completely detached divertor which we assume happens at $T_{osp} = 1$. Just to demonstrate the proof of principals we choose $T_{TC} = 10$ and $K = 4$. The results of our 2D simulation for DIII-D-like geometry and $Q_{edge} = 2$ MW demonstrated that for the case with no feedback of divertor conditions on TC, divertor plasma temperature was gradually decreasing function of plasma density at edge-core interface. However, with a "positive feedback" of TC on T_{osp}, an abrupt reduction of divertor temperature occurs when T_{osp} drops below T_{TC} and outer divertor becomes virtually detached (see Fig. 2). We note that an increase of N_D for the fixed TC does not result in the bifurcation phenomena [12].

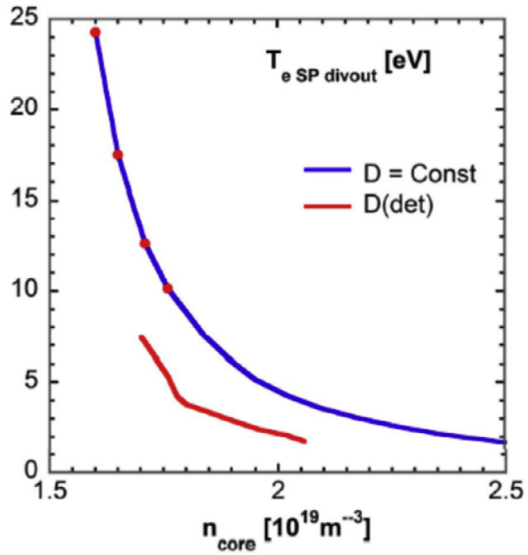

Fig. 2. Dependence of plasma temperature at the outer strike-point on core plasma density for a constant transport coefficients (blue) and transport coefficients with a "positive feedback" of detachment (labeled as "D(det)", red). (For interpretation of the references to colour in this figure legend, the reader is referred to the web version of this article.)

Similar effect can be related to the plasma recycling process on the PFCs. Even though in the simulations plasma recycling on the PFCs is often described by some albedo, which provide an instantaneous flux of neutrals back to the volume, in practice, recycling is a very complex and still poorly understood number of the processes which include reflection, absorption on the surface, penetration of hydrogen into lattice, transport of hydrogenic species in the wall material, desorption from the surface, etc. All of these processes are sensitive to both energy of the particles impinging on the surface as well as the temperature and constituency of the near surface material layer. Therefore: i) there is some delay between the time particle impinging on the surface and the time it comes back to the volume, and ii) the variation of both surface condition of the PFCs and plasma parameters can break the delicate balance of the particle flux to and from the PFCs, which taking into account extremely large amount of hydrogen usually stored in the PFCs in comparison with total inventory of hydrogen in the discharge (in particular in Carbon PFCs) [13], can have a devastating effect on edge plasma performance. This is what indeed happen in a long pulse discharges described in Ref. [3], where increasing temperature of divertor tiles were promoting thermal desorption of hydrogen, which, finally, caused abrupt transition to deep detachment and MARFE formation.

3. Current convective instability of detached plasma

In this Section we present a plausible explanation of origin of radiation fluctuations in the AUG tokamak reported in Ref. [5]. These fluctuations, with the frequencies ~10 kHz, were observed for the case where only inner divertor was detached and both detachment and radiation fronts were located close to the X-point. However, fluctuations disappear when the outer divertor also detaches.

We show that the origin of the radiation oscillations can be attribute to current convective instability [14] developing in cold plasma in inner divertor. It is widely accepted that current convective instability, which in tokamak related literature is called the

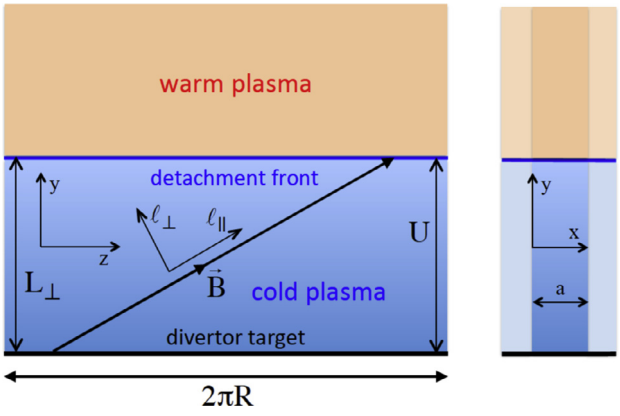

Fig. 3. Schematic view of inner divertor plasma in a slab approximation.

"rippling mode" (e.g. see Ref. [15–17]), does not play significant role in anomalous plasma transport in hot core region due to high plasma heat conduction along the magnetic field and magnetic shear effect [18], although it might be important in relatively cold edge plasma [16,17]. However, on the closed flux surfaces the parallel electric field driving the parallel current causing the rippling instability is small, $\sim 10^{-3}$V/cm, meanwhile in the scrape off layer (SOL) plasma (see Fig. 3) it can be much larger, ~ 1 V/cm. The reason for this is that in the SOL the parallel current is largely driven by the difference of electron temperatures $T_d^{(out)}$ and $T_d^{(in)}$ in the vicinity of outer and inner divertor targets respectively [19]. This is because the drop of electrostatic potential through the sheath is $\sim 4T_d$ for the case where no current flows through the sheath. For the case where $T_d^{(out)} \neq T_d^{(in)}$ and inner and outer divertor targets are electrically connected (which is the case in current tokamaks) the current will flow through the SOL plasma. The magnitude of the current will be determined by the difference $T_d^{(out)} - T_d^{(in)}$ and the SOL plasma resistivity [19]. When inner (outer) divertor is detached (attached) we have $T_d^{(out)} >> T_d^{(in)}$ and the SOL resistivity is largely determined by the resistivity of cold, ~ 1 eV, plasma in inner divertor. As a result, virtually the whole potential drop, $U \sim 4T_d^{(out)}$, driving the SOL current will be localized within detached plasma, creating large parallel electric field. This high electric field in the SOL, in conjunction with a very low plasma temperature in detached divertor region, which strongly decreases stabilizing role of electron heat conduction, can cause robust current convective instability in detached plasma.

Fluctuation of plasma parameters, including pressure, in detached inner divertor will cause the bursts of plasma outflow from the radiation region (located beyond the detachment front) and subsequent fluctuation of the radiation loss. Once the outer divertor also detaches, a strong asymmetry between $T_d^{(out)}$ and $T_d^{(in)}$, causing large potential drop through inner divertor, disappears. As a result, when both divertors are detached, the drive for the current convective instability in inner divertor and subsequent fluctuations of the radiation loss does not exist anymore.

To make some quantitative estimates we consider a slab approximation for detached inner divertor plasma assuming periodic boundary conditions along the "toroidal" z-coordinate (see Fig. 3). In poloidal direction cold ($T_{cold} \sim$ few eV, we assume that electron and ion temperatures are equal) plasma region extends at the distance $L_\perp \sim 10$ cm up to detachment front where it contacts with warm ($\sim$ few tens of eV) SOL plasma. The characteristic scale-length of temperature and, therefore, conductivity variation along "radial" coordinate x we assume to be a ~ 2 cm. The potential drop, U, between detachment front and the target we assume to be $eU \equiv U_e \sim 4T_d^{(out)} \sim 30$ eV $>> T_{cold} \sim 3$ eV, where e is the electron charge. In our estimates we will assume that plasma density in detached region, $n_{det} \sim 3 \cdot 10^{14}$ cm^{-3}, the magnitude of magnetic fields $B_z \sim 3$ T and $B_y \sim 0.1 \times B_z$, and the effective magnetic shear length $L_s \sim 1$ m (we assume that detachment front is not too close to the X-point where magnetic shear is much stronger).

First we notice that the potential drop through detached plasma causes E × B drift in radial direction. As a result, detached plasma parameters are determined by two competing processes: radial E × B drift, which is characterized by the frequency $\nu_{E\times B}^{(x)} \approx (U_e/M)/(\Omega_i a L_\perp)$ (where M and Ω_i are the ion mass and gyrofrequency) and parallel plasma flow having characteristic time-scale $\tau_{||} \approx L_\perp/(b_y\sqrt{T_{cold}/M})$, where $\vec{b} = \vec{B}/B$ ($b_z^2 >> b_y^2$) and $L_{||} = L_\perp/|b_y|$. For the parameters of the interest we have $\tau_{||}\nu_{E\times B}^{(x)} \approx 0.3 \lesssim 1$, so that in a ballpark we can assume rather well defined kernel of detached plasma with electron temperature and, therefore, electric conductivity significantly different from surrounding plasma, which is shown in light blue color in Fig. 3.

Then, neglecting the effects of parallel electron heat conduction and magnetic shear (corresponding estimates will be given below) and assuming that the divergence of electric current is zero we find the following linearized equation for electrostatic potential $\Phi \propto \varphi(\vec{r})e^{-i\omega t}$ describing the current-convective instability (e.g. see Ref. [14]):

$$\frac{\omega}{\omega_A}\nabla_\perp^2\varphi + i\nabla_{||}\left\{\frac{\omega_\sigma}{\omega}(\vec{e}_x \times \vec{b})\cdot\nabla + \nabla_{||}\right\}\varphi = 0, \quad (3)$$

where $\omega_A = 4\pi\sigma_0(V_A/c)^2$, $\omega_\sigma = -i(cE_{||}/B)[d\ell n(\sigma_0)/dx]$, $E_{||}$is the parallel component of electric field, $\sigma_0(x)$ is the electric conductivity, c and $V_A = B/\sqrt{4\pi M n_{det}}$ are the light and the Alfven speeds. We notice that for the parameters of interest $\omega_A \sim 10^{11}s^{-1} >> |\omega_\sigma| \sim 10^3 s^{-1}$ (we assume here that $|d\ell n(\sigma_0)/dx| \approx 2/a$).

Generally speaking frequency ω should be found as an eigenvalue of the solution of Eq. (3) by using periodic boundary conditions along "toroidal coordinate z and a proper boundary condition along "poloidal" coordinate y. However, due to the lack of space a complete analysis will be considered in details elsewhere. Here we present just our main findings.

First we consider the solution of Eq. (3) in the eikonal approximation assuming $\varphi(\vec{r}) \propto exp(ik_\perp\ell_\perp + ik_{||}\ell_{||} + ik_x x)$, where the coordinates $\ell_\perp$ and $\ell_{||}$ are shown in Fig. 3 while $k_\perp$, $k_{||}$, and k_x are the corresponding wave numbers. Then, from Eq. (3) we find the following dispersion equation

$$-i\frac{\omega}{\omega_A}\frac{k_\perp^2 + k_x^2}{k_{||}^2} + \frac{\omega_\sigma}{\omega}\frac{k_\perp}{k_{||}} + 1 = 0. \quad (4)$$

First we consider the case $k_x = 0$. Then from Eq. (4) we find that for $|k_\perp/k_{||}| < (\omega_A/|\omega_\sigma|)^{1/3}$ the first term in Eq. (3) is small so the growth rate of the instability, γ, increases with increasing $|k_\perp/k_{||}|$ as $\omega = i\gamma = i|\omega_\sigma k_\perp/k_{||}|$, reaching maximum $\gamma \approx |Re(\omega)| \approx \omega_{max}^{(A)} \equiv (\omega_A|\omega_\sigma|^2)^{1/3}$ at $|k_\perp/k_{||}| \approx |k_\perp/k_{||}|_{max}^{(A)} \equiv (\omega_A/|\omega_\sigma|)^{1/3}$, when all terms in Eq. (4) are the of same order, and then decreases as $\gamma \approx |Re(\omega)| \propto (|k_\perp/k_{||}|)^{-1/3}$ with further increasing $|k_\perp/k_{||}| > |k_\perp/k_{||}|_{max}^{(A)}$ where only first and second terms in Eq. (4) matter.

However, in practice, it appears that the stabilizing effects of parallel electron heat conduction and magnetic shear bound the range of possible growth rates. Moreover, finite k_x may also alter the growth rate. The effect of parallel electron heat conduction can be neglected for $\gamma > \alpha_e k_{||}^2$, where α_e is the electron heat diffusivity. Taking as an estimate $|k_{||}| \approx 2\pi/L_{||}$ we find that $\alpha_e k_{||}^2 \sim 2 \cdot 10^4 s^{-1} << \omega_{max}^{(A)}$ and potentially the instability can develop. As a matter of fact, the threshold for the instability is determined by the inequality $(k_\perp)_{thr} \gtrsim \alpha_e k_{||}^3/|\omega_\sigma|$, which for $|k_{||}| \approx 2\pi/L_{||}$ corresponds to $(\lambda_\perp)_{thr} = 2\pi(k_\perp)_{thr}^{-1} \lesssim 5$ cm. Let us now discuss an impact of k_x. Based on preceding analysis, we find that within the eikonal

approximation any sizable effect of k_x on the growth rate is possible for $k_x^2 \tilde{>} (k_\perp^2)^{(A)}_{max}$. Estimating $k_x^2 \approx (2\pi/a)^2$ and noticing that $\lambda^{(A)}_{max} \sim 0.2$ cm << a ~ 2 cm, we conclude that within an eikonal approximation k_x does not alter the results of our analysis of the instability growth rate.

Now we consider an impact of the shear of the magnetic field. As we have mentioned above, both spatial localization and the growth rate of the "rippling mode" crucially depend on magnetic shear [15–18]. However, while for the "rippling mode" developing on some closed rational magnetic flux surface the effective length of the magnetic field line and, therefore the stabilizing effect of parallel heat conduction is determined solely by the magnetic shear, in our case the length of the magnetic field line between the target and detachment front does not varies much. Indeed, assuming that $b_y(x) = b_y(0)\{1 + x/L_s\}$ we find that the variation of $L_{||}(x) \approx L_\perp/|b_y(x)|$ within unstable region is about $\delta L_{||} \approx (a/2)(L_{||}/L_s) << L_{||}$ (we assume here that $L_{||} \approx L_s \approx 1$ m). However, the solution of the eigenvalue problem shows that the maximum growth rate is reached by maximizing the ratio of effective perpendicular and parallel wave numbers, where $(k_\perp)_{eff} \approx k_n/b_y = n/b_y R$ (n is the integer number) and $(k_{||}^2)_{eff} = |b_y \eta_{(\pm)} + i b_z k_n|^2$ (where $\eta_{(\pm)}$ plays the role of poloidal wave number $\vec{b} = \vec{B}/B$, $b_z^2 >> b_y^2$, $k_n = n/R$ and n is the toroidal mode number). As a result, maximum growth rate is reached for $\eta_{(\pm)} \approx -i(b_z/b_y)k_n + i\delta_m k_m (k_m = 2\pi m/L_\perp$, m is the integer number, and $\delta_m \sim 1$) which almost cancels large term $ib_z k_n$ in the expression for $(k_{||}^2)_{eff}$. However, taking into account the effect of magnetic shear on the variation of $\eta_{(\pm)}$ with x, we find $(k_{||}^2)_{eff} \approx |\{x/[b_y(0)L_s]\}k_n + \delta_m k_m|^2$ so that a strong increase of effective parallel wave number, caused by magnetic shear and resulting in the reduction of the growth rate, starts at $|k_n/(b_y k_m)| \tilde{>} |k_\perp/k_{||}|_{sh} \equiv 2L_s/a$. We notice that for the parameters of interest $|k_\perp/k_{||}|_{sh} < |k_\perp/k_{||}|^{(A)}_{max}$ and the maximum growth rate, γ_{max}, is, actually, determined by the magnetic shear effect, which gives $\gamma_{max} \approx (2L_s/a)|\omega_\sigma| \sim 10^5 s^{-1}$. Assuming $|k_{||}|_{sh} \approx 2\pi/L_{||}$, we find the low bound of the current convective instability wavelength $|\lambda_\perp|_{sh} \approx (a/2)(L_{||}/L_s) \sim 1$ cm. Thus, we find that the development of the aperiodic current convective instability is limited within the range of the growth rates $\gamma \sim 10^4 \div 10^5 s^{-1}$. In a nonlinear regime one can expect the transformation of the aperiodic current convective instability in a turbulent oscillations with the frequency $\omega \sim \gamma$, which is in a reasonable agreement with experimental data showing ~ 10 kHz oscillation frequency of the radiation loss. However, numerical simulations are needed to explore a nonlinear regime of current convective instability and give some guidance on the magnitude and spectrum of the fluctuations.

4. Self-sustained oscillations driven by impurity radiation

It is usually assumed that the radiative condensation instability results in establishing a new steady-state equilibrium with inhomogeneous plasma parameters, which magnetic fusion research is usually associated with MARFE (e.g. see Ref. [20] and the references therein). However, more detail studies demonstrate that an impact of thermal force, pushing radiative impurities toward high plasma temperature region, causes slowly traveling modes in linear theory [21], and regular self-sustained oscillations (SSO) of plasma parameters in a non-linear phase [8]. However, so far the main features of these SSO were not clear. Here we present our results of analytic and numerical studies elucidating the main physics of the SSO.

We address the SSO driven by impurity radiation by using simple model describing the dynamics of main plasma and impurity as well as the energy balance along the closed magnetic field line of length L_0. For simplicity, following Ref. [21], we assume: i) the impurity density is small and does not alter the dynamics of main plasma, ii) all species have the same temperature, and iii) ignore source/sink of main plasma and impurity particles. Then in normalized units our governing equations are:

$$\partial_\tau \eta + \partial_\xi(\eta w) = 0, \qquad \eta(\partial_\tau w + w\partial_\xi w) = -\partial_\xi(\eta\vartheta) + \ell_I^{-1}\partial_\xi(\eta\vartheta^{5/2}\partial_\xi w), \tag{5}$$

$$\partial_\tau \eta_I + \partial_\xi(\eta_I w_I) = 0, \quad \frac{2}{\mu}\eta_I(\partial_\tau w_I + w_I\partial_\xi w_I) = \alpha_T\eta_I\partial_\xi\vartheta - \vartheta\partial_\xi\eta_I + \frac{Z_I^2(\vartheta)}{\vartheta^{3/2}}\ell_I\eta_I\eta(w - w_I), \tag{6}$$

$$3\eta(\partial_\tau\vartheta + w\partial_\xi\vartheta) = -2\eta\vartheta\,\partial_\xi w + \mu_e^{-1/2}\ell_e^{-1}\partial_\xi(\vartheta^{5/2}\partial_\xi\vartheta) + Q_0 - \eta\eta_I R(\vartheta), \tag{7}$$

where η (η_I) is the plasma (impurity) density normalized on it's initially homogeneous density $\bar{n}$ ($\bar{n}_I$), ξ is the parallel coordinate normalized on L_0, w (w_I) is plasma (impurity) velocity normalized on $(2T_0/M)^{1/2}$ and M (M_I) is the mass of main (impurity) ions, while T_0 is some normalization temperature, $\vartheta = T/T_0$, τ is the time normalized on $L_0/(2T_0/M)^{1/2}$, $\mu = M/M_I$ and $\mu_e = m/M$, m is the electron mass, $Z_I(\vartheta)$ and $\alpha_T(\vartheta) \approx 2.2Z_I^2(\vartheta) \equiv \alpha_0 Z_I^2(\vartheta)$ are impurity charge and thermal force coefficient (we assume that $Z_I(\vartheta) > 1$ so that $\alpha_T >> 1$), ℓ_I (ℓ_e) is the ratio of L_0 to effective mean free path of main ions (electrons) till collisions with impurity ions (main ions) assuming that they are singly charged and density is equal to $\bar{n}$ (we notice that the applicability of fluid equations requires $\ell_I >> 1$ and $\ell_e >> 1$), $R(\vartheta)$ is the impurity cooling function, and Q_0 is the normalized heating term.

Linearizing Eqs. (5–7) over homogeneous stationary solution we arrive to the dispersion equation found in Ref. [20]. Next we examine the availability of stationary, but inhomogeneous solutions. After some algebra we arrive to the following equations

$$\frac{(\vartheta^{5/2}\partial_\xi\vartheta)^2}{2\mu_e^{1/2}\ell_e} = G(\vartheta) - G(\vartheta_{min}),$$

$$G(\vartheta) = G_0\int_0^\vartheta d\vartheta' R(\vartheta')\vartheta'^{3/2} e^{\int_0^{\vartheta'} d\vartheta''\alpha_T(\vartheta'')/\vartheta''} - \frac{2}{7}Q_0\vartheta^{7/2}, \tag{8}$$

where ϑ_{min} is the minimal value of normalized temperature, and

$$G_0 = \left\{\int_0^1 d\xi\, exp\left(\int_0^{\vartheta(\xi)} d\vartheta'\alpha_T(\vartheta')/\vartheta'\right)\right\}^{-1}\left\{\int_0^1 d\xi/\vartheta(\xi)\right\}^{-1}. \tag{9}$$

Since we have the periodic boundary conditions at $\xi \in [0,1]$ we should have at least one maximum of $\vartheta(\xi)$, ϑ_{max}, where, as it follows from (8), we should have $G(\vartheta_{max}) = G(\vartheta_{min})$. However, due to thermal force effect (recall that $\alpha_T >> 1$) an extremely large exponential factor in the expression for $G(\vartheta)$ results in a very fast growth of the first term virtually for all reasonable functions $R(\vartheta)$. Therefore, the condition $G(\vartheta_{max}) = G(\vartheta_{min})$ can only be satisfied for relatively small ϑ where the second term dominates. But for this case $G(\vartheta) - G(\vartheta_{min}) < 0$ and the differential equation for $\vartheta(\xi)$ in (8) is meaningless. Thus, for this case there is no stationary inhomogeneous solution of Eqs. (5–7) possible and plasma parameters will continually vary in time.

To study time dependent solution we solve Eqs. (5–7) numerically taking $R(\vartheta) = R_0\vartheta^3/(1+\vartheta^3)^2$ for $\vartheta \le 1$ and $R(\vartheta) = R_0/4$ for $\vartheta > 1$. We choose $\ell_I = \ell_e = 10$, $\mu = 0.05$, $\mu_e = 5.5 \times 10^{-4}$, $Z_I(\vartheta) = Z_0\vartheta$, $Z_0 = 3$, $R_0 = 360.9$, and $Q_0 = 90$. Stationary plasma temperature for our case is close to 1. Linear analysis shows that for these parameters only first mode is unstable. We seed small temperature perturbation and observe that after some initial stage, a nonlinear

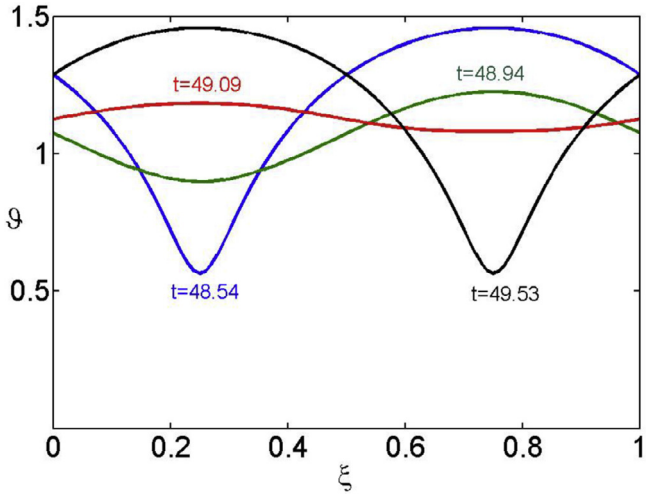

Fig. 4. Time evolution of plasma temperature profile in developed self-sustained oscillations.

SSO develop with a period ~1 and the amplitude of temperature variation ~0.5. The time variation of $\vartheta(\xi)$ profile over a half of a period is shown in Fig. 4. More detail discussion of the results of numerical simulations will be presented elsewhere.

5. Conclusions

Thus we find that: i) Unlike some simplified models, dealing with an impact of impurity radiation on the transition to detachment, 2D simulation of dynamics of plasma and impurity shows no bifurcation-like transition into detached regime. However, bifurcation-like transition becomes possible for the case where cross-field plasma transport increases while detachment is approaching (e.g. with decreasing plasma temperature in divertor). Absorption/desorption processes on the PFCs can cause similar effect on the transition to detachment. We note that the increase of cross-field plasma transport in detached plasmas was recently observed in experiments [9]. ii) The fluctuations of impurity radiation, observed experimentally [5] for the case where inner divertor is detached while the outer one is not, and the absence of these fluctuations, for the case where both divertor are detached, can be explained by the development/stabilization of current-convective instability in inner divertor plasma. iii) Radiative-condensation instability not necessarily results in establishing of inhomogeneous along the magnetic field but stationary plasma parameter distribution. Due to an impact of the thermal force, acting on impurity ions, the nonlinear phase of this instability can end up in the development of self-sustained oscillations of plasma parameters.

Acknowledgements

This material is based upon the work supported by the U.S. Department of Energy, Office of Science, Office of Fusion Energy Sciences under Award No. DE-FG02-04ER54739 at UCSD, and the Russian Ministry of Education and Science under Grant No. 14.Y26.31.0008 at MEPhI.

References

[1] ITER Physics Basis, Chapter 4: power and particle control, Nucl. Fusion 39 (1999) 2391–2469.
[2] S.I. Krasheninnikov, A.S. Kukushkin, A.A. Pshenov, Divertor plasma detachment, Phys. Plasma 23 (2016) 055602.
[3] T. Fujita, the JT-60 team, Steady state operation research in JT-60 U with extended pulse length, Nucl. Fusion 46 (2006) S3–S12 T. Nakano, N. Asakura, H. Takenaga, H. Kubo, Y. Miura, K. Shimizu, S. Konoshima, K. Masaki, S. Higashijima and the JT-60 team, Impact of wall saturation on particle control in long and high-power-heated discharges in JT-60 U, Nucl. Fusion 46 (2006) 626-634.
[4] A.G. McLean, A.W. Leonard, M.A. Makowski, M. Groth, S.L. Allen, J.A. Boedo, B.D. Bray, A.R. Briesemeister, T.N. Carlstrom, D. Eldon, M.E. Fenstermacher, D.N. Hill, C.J. Lasnier, C. Liu, T.H. Osborne, T.W. Petrie, V.A. Soukhanovskii, P.C. Stangeby, C. Tsui, E.A. Unterberg, J.G. Watkins, Electron pressure balance in the SOL through the transition to detachment, J. Nucl. Mater. 463 (2015) 533–536.
[5] S. Potzel, M. Wischmeier, M. Bernert, R. Dux, H.W. Muller, A. Scarabosio, the ASDEX Upgrade Team, A new experimental classification of divertor detachment in ASDEX Upgrade, Nucl. Fusion 54 (2014) 013001.
[6] I.H. Hutchinson, Thermal front analysis of detached divertors and MARFEs, Nucl. Fusion 34 (1994) 1337–1348.
[7] S.I. Krasheninnikov, Two-dimensional effects in plasma radiation fronts and radiation front jumps in tokamak divertor plasmas, Phys. Plasmas 4 (1997) 3741–3743.
[8] R.D. Smirnov, A.S. Kukushkin, S.I. Krasheninnikov, A.Yu. Pigarov, T.D. Rognlien, Impurity-induced divertor plasma oscillations, Phys. Plasmas 23 (2016) 012503.
[9] H.J. Sun, E. Wolfrum, T. Eich, B. Kurzan, S. Potzel, U. Stroth, the ASDEX Upgrade Team, Study of near scrape-off layer (SOL) temperature and density gradient lengths with Thomson scattering, Plasma Phys. Contr. Fusion 57 (2015) 125011 D. Carralero, G. Birkenmeier, H.W. Muller, P. Manz, P. deMarne, S.H. Muller, F. Reimold, U. Stroth, M. Wischmeier, E. Wolfrum and The ASDEX Upgrade Team, An experimental investigation of the high density transition of the scrape-off layer transport in ASDEX Upgrade, Nucl. Fusion 54 (2014) 123005.
[10] S.I. Krasheninnikov, M. Rensink, T.D. Rognlien, A.S. Kukushkin, J.A. Goetz, B. LaBombard, B. Lipschultz, J.L. Terry, M. Umansky, Stability of the detachment front in a tokamak divertor, J. Nucl. Mater. 266-269 (1999) 251–257.
[11] A.S. Kukushkin, H.D. Pacher, V. Kotov, G.W. Pacher, D. Reiter, Finalizing the ITER divertor design: The key role of SOLPS modeling, Fusion Eng. Des. 86 (2011) 2865–2873.
[12] A.A. Pshenov, A.S. Kukushkin, S.I. Krasheninnikov, Energy Balance in Plasma Detachment, this Conference, Poster P1.40, submitted to the J. Nucl. Mater. Energy.
[13] J. Roth, E. Tsitrone, A. Loarte, Th. Loarer, G. Counsell, R. Neu, V. Philipps, S. Brezinsek, M. Lehnen, P. Coad, Ch. Grisolia, K. Schmid, K. Krieger, A. Kallenbach, B. Lipschultz, R. Doerner, R. Causey, V. Alimov, W. Shu, O. Ogorodnikova, A. Kirschner, G. Federici, A. Kukushkin, EFDA PWI Task Force, ITER PWI Team, Fusion for Energy, ITPA SOL/DIV, Recent analysis of key plasma wall interactions issues for ITER, J. Nucl. Mater. 390-391 (2009) 1–9.
[14] B.B. Kadomtsev, A.V. Nedospasov, J. Nucl. Energy Part C 1 (1960) 230.
[15] H.P. Furth, J. Killeen, M.N. Rosenbluth, Finite-resistivity instabilities of a sheet pinch, Phys. Fluids 6 (1963) 459–484.
[16] B.A. Carreras, P.W. Gaffney, H.R. Hicks, J.D. Callen, Rippling modes in the edge of a tokamak plasma, Phys. Fluids 25 (1982) 1231–1240.
[17] A.B. Hassam, J.F. Drake, The rippling instability, Phys. Fluids 26 (1983) 133–138.
[18] B.B. Kadomtsev, O.P. Pogutse, in: M A Leontovich (Ed.), Reviews of Plasma Physics, Vol. 5, Consultants Bureau, New York, 1970, p. 249.
[19] G.M. Staebler, F.L. Hinton, Currents in the scrape-off layer of diverted tokamaks, Nucl. Fusion 29 (1989) 1820–1824.
[20] D. McCarthy, J.F. Drake, Nonlinear behavior of the radiative condensation instability, Phys. Fluids B 3 (1991) 22–25.
[21] D.Kh. Morozov, J.J.E. Herrera, Slow thermal waves in impurity seeded radiative plasmas, Phys. Rev. Lett. 76 (1996) 760–763.